Case study of a back up dam built to bear dynamical loadings from tailings in Brazil

G. O. F. Santos
Civil Engineer MSc Geotechnical Engineering – Fonntes Geotécnica
C. F. Bora
Civil Engineer MSc Geotechnical Engineering – Vale S.A.
F. Pereira
Civil Engineer MSc Geotechnical Engineering – Vale S.A.
M. M. M. Fontes
Civil Engineer MSc Geotechnical Engineering - Fonntes Geotécnica
M. M. Futai
Professor of the Geotechnical Engineering Department – Escola Politécnica da USP
I. Viel
Civil Engineer MSc Geotechnical Engineering – Fonntes Geotécnica
B. C. F. Novais
Geologist – Fonntes Geotécnica

ABSTRACT

This article reports a case study from a Back Up Dam (BUD) built to withstand dynamical loadings that could happen due to a failure of two iron tailings dams built by the upstream method. The back up dam is composed of lines of piles with concrete cast between them. Analysis by Finite Element Method (FEM) of the loaded structure was performed to understand the loadings, the order of displacements and angular deflections to which the Back Up Dam would be subjected.

Key words: *Back Up Dam (BUD), Finite Element Method (FEM), Upstream method*

1. Introduction

The Term of Reference SEMAD/FEAM no. 2.784, published on March 21st, 2019, made it imperative to develop a Back Up Dam (BUD) during the decommissioning of tailing dams built by upstream altering in order to halt the flow of the material that could behave in a liquefied state during failure and ensure the safety of regions downstream that would be affected.

Since the tailings behave with low to no resistance to move during liquefaction, they could reach heights to several meters. In a restricted physical space to build a structure, a good alternative would be the usage of steel tubular piles. Steel would allow for a slender structure due to its relatively low self-loading and low possibility of buckling due to its high resistance and low deformability. Pile driving equipment of BUD's should generate low vibrations in the soil media in order not to promote dynamic loadings that could trigger an increase in pore pressure and liquefaction in contractile materials with the dam. Taking that into consideration, SILENT PILER™ equipment of GIKEN LTD. would be adequate to use under these circumstances, once the induced stresses on the media are located in a restricted area and very low, with loadings of Rotational Torque applied to soft layers and Press-in force applied to stiff layers. The equipment also applies an Extraction Force during pile driving in order to reduce stresses induced by machinery. Finally, the equipment utilizes a Water Jet Volume on the soil during a Rotational Torque in order to promote a resistance reduction in the soil located inside the pile and facilitate pile driving. **Figure 1** provides a simplified illustration of the pile driving procedure of SILENT PILER™.

A BUD was built in Brazil, consisting of two lines of steel tubular piles embedded in lateralized residual soil. Concrete was cast between two lines of piles in order to let stresses be transmitted between them. The structure was designed according to Ultimate Limit State Design to evaluate structural forces acting upon it. **Figure 2** shows the plan view of the structure.

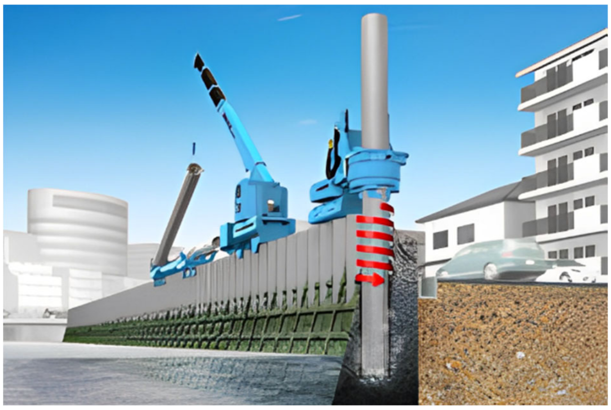

Figure 1 Pile driving procedure of SILENT PILER™

There were no adequate deformability criteria for this structure since the typical structures are not subjected to such intense exceptional loading. Maximum allowable displacement methods are normally suggested in standards for Serviceability Limit State. The standard NBR6118 (2014) established for structural elements, as a sensory acceptability, a maximum displacement/height ratio of 1/250. In the geotechnical field, Japan Road Association (2009) establishes a maximum displacement at the top of the retaining wall of 3% of the embedded depth. Nevertheless, these limits are not Ultimate State Limits.

Santos and Futai (2022) developed Ultimate State Limit criteria for angular deflections of steel tubular piles that would be used as BUD's. The acceptable value allowed was 3,6%. The allowable angular deflection in this case study was set at 3%.

2. Methodology

The BUD site is situated on a hill within a watershed supported by a thick layer of weathered gneiss, which generated a soil profile of residual lateralized soils. The half space has an improvement of resistance with depth, with geomechanical behaviors of higher classes. Therefore, the layers of the geological profile are distinguished by how weathered the layer has been, with residual soil as highly weathered soil, young residual soil as intermediately weathered soil and saprolite as lowly weathered soil, with geomechanical behavior more akin of the rock. **Figure 3** presents geological-geotechnical profile of the soil in a cross-section parallel of the Back Up Dam.

The piles used in the BUD are steel tubular piles ASTM A572 GR50, with a diameter of 1000mm and a thickness of 19mm. Spacing between piles along the longitudinal axis is 18cm. Geometrical parameters of the retaining wall are reduced by a correction factor that accounts for Plain Strain analysis, considering the sum of the diameter and spacing between piles (1.18m), in order to obtain resistance by meter. Maximum bending moment of the piles would be connected to steel's yielding stress, as shown on **Eq. (1)**.

$$M_{max} = \frac{\sigma_{max} * I_c}{y} = \frac{\sigma_{max}}{y} * \frac{\pi\,(R_{ext}{}^4 - R_{int}{}^4)}{4(D_{ext}+e)} \tag{1}$$

As $\sigma_{max} =$ Steel's yielding stress (kPa); $y =$ maximum distances between stresses elements and the structure's center of gravity (m); $I_c =$ moment of inertia to plane strain analysis (m^4); R_{ext}= pile's external radius (m); $R_{int} =$ pile's internal radius; $D_{ext} =$ pile's external diameter; $e =$ spacing between piles (m).

The area of the tubular piles is also adjusted to consider plane strain conditions, as shown on **Eq. (2)**.

$$A_c = \frac{\pi\,(R_{ext}{}^2 - R_{int}{}^2)}{(D_{ext}+e)} \tag{2}$$

Table 1 presents the properties of the pile element in stress-strain analysis. Stress-strain analysis by FEM is evaluated by loading stages (initial condition, BUD installation, tailing loading maximum impact applied on BUD and tailing retaining stage) in order to compare the

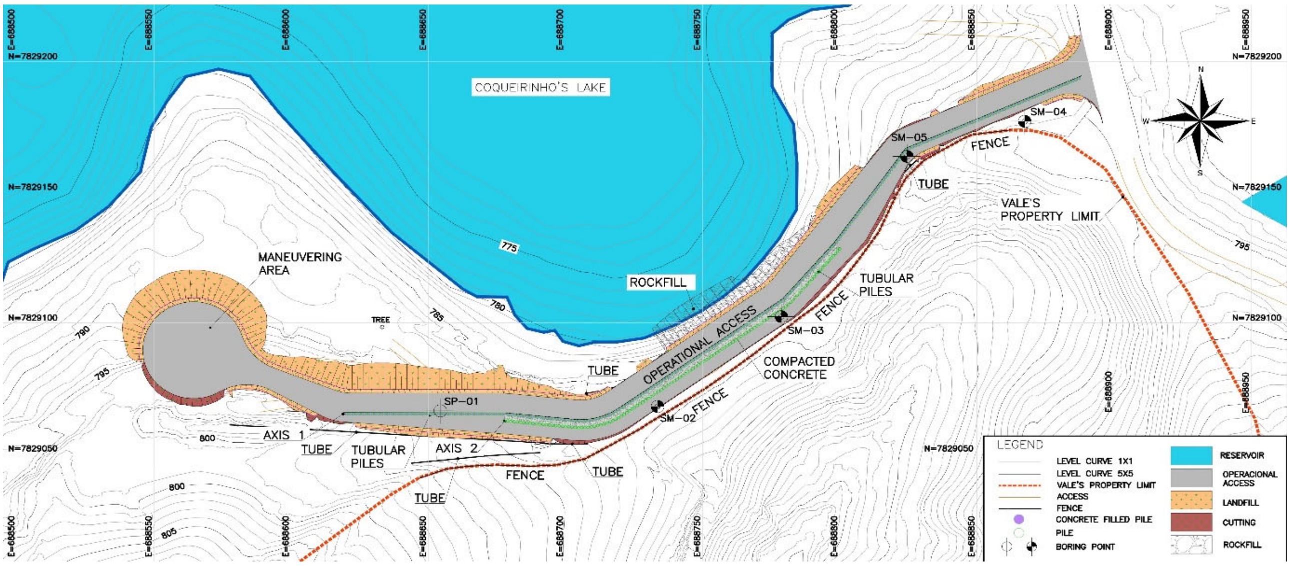

Figure 2 Plan view of the BUD consisting of steel tubular piles

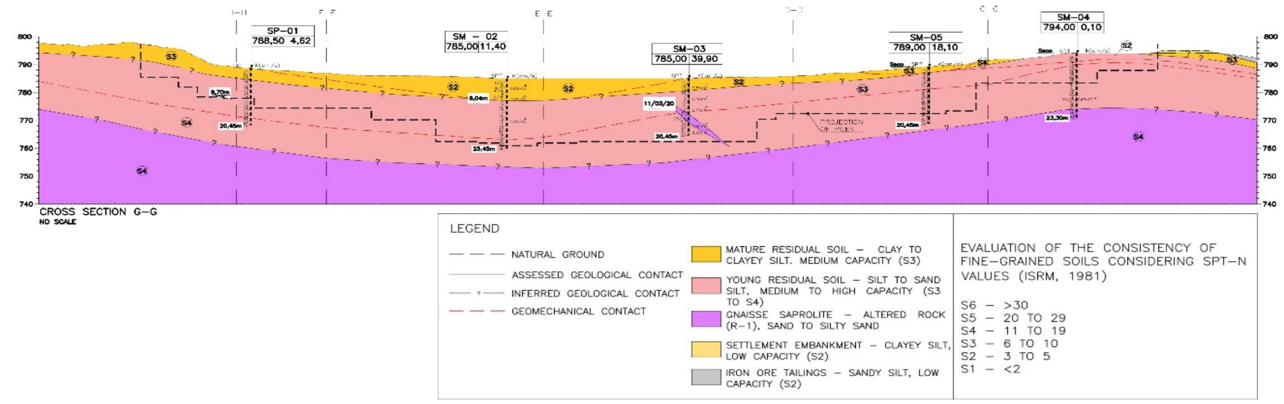

Figure 3 Geological profile of the cross-section parallel to the Back Up Dam

loading stages to the initial stage and generate the differential displacement between stages.

In addition, information of the surrounding environment, such as the existence of mountain, sea, river, and so on, should also be written here if necessary.

The initial stresses on the soil are created by a gravity stage, considering topography of the media. The boundary conditions on x and y axis to $y_{minimum}$ (avoiding errors in generalized media displacement) and restrained displacements on x axis to $x_{minimum}$ and $x_{maximum}$.

The initial ratio between effective horizontal stresses and effective vertical stresses for all materials is set at 0.7. The elastoplastic behavior is set to all soil materials, with the same resistance parameters before and after the failure. The soils are modeled using the Mohr Coulomb failing criteria.

The soil parameters were set based on field investigation data (SPT, permeability tests) and laboratory analysis (tri-axial tests, consolidated undrained tests on mature and young residual soils). **Table 2** presents the soils' parameters used in the FEM analysis. The permeability between piles is adjusted by an area factor in order to account for the smaller area available between piles after pile driving.

In order to evaluate the impact loadings acting on BUD, a 3D Finite Element Method software that would simulate the dynamics of the failing tailing was used. The read geometry and volumes of the failing dam and BUD could be better represented in the 3D FEM method, and it would vary greatly the loading distribution that would act on the structure.

Table 1. Properties of the pile element of stress-strain analysis

Pile parameters (2D analysis)	
Steel type	ASTM A572 GR50
Yielding stress (MPa)	345
Beam type	Timoshenko
External diameter (mm)	1000
Thickness (mm)	19
Spacing between piles (cm)	1.8
Plane Strain Area (1mm internal and external corrosion) (m^2)	4.44E-02
Plane strain moment of inertia (1mm internal and external corrosion) (m^4)	5.34E-03
Maximum bending moment (Safety factor=1) (kNm)	3686.5
Maximum bending moment (Safety factor=1.5) (kNm)	2457.7

Table 2. Properties of the pile element of stress-strain analysis

Soil layer	Specific weight (kN/m^3)	Cohesion (kPa)	Friction angle (°)	Young modulus (kPa)	K (m/s)	K between piles (m/s)	Color
Embankment	20	9	22	7900	2.27e-07	3.46E-08	
Mature residual soil	16	15	32	6880	6.21e-08	9.47E-09	
Young residual soil	17	32.5	22	16380	1.03e-08	1.57E-09	
Young residual soil S4	17	32.5	34		1.03e-08	1.57E-09	
Gneiss saprolite	20	10.5	35	66000	5.53e-08	8.44E-09	
Undrained iron ore tailing	23	0	12	6000	3.47e-06	-	
Drained iron ore tailing	24	0	32	9000	3.47e-06	-	

Flow3D (FlowScience) is a 3D Finite Element Method software that can generate an output of pressures over time on its elements. The tailing of the dam on the software was modeled using the Bingham constitutive model, with a dynamic viscosity of 1Pa*s and failing shear stress of 120 Pa and specific weight of 24 kN/m³. The particle size distribution curve of the tailing dams is presented in **Figure 4** and serves as a good indicator of potential liquefaction. Should the two dams fail due to liquefaction triggering, a volume of 4.26 Mm³ of tailings would be mobilized.

The geometry considered in the 3D model is presented in **Figure 5**. The elements have an average size of 3m.

The results of the pressure forces on the model as an output is presented in **Figure 6**. The pressure computed at different heights of the BUD across various cross-sections of the structure. The distribution of pressures over time at the critical cross-section is presented in **Figure 7**. The most significant loading distributions are presented in **Figure 8**.

Cross-section E-E is the most critical cross-section in terms of tailing loadings acting on the BUD. It required two lines of piles to be built, connected by casted concrete in the field, in order to better transmit stresses between piles and ensure the rigid behavior of the structure. **Figure 9** presents the geological profile of the cross-section E-E and **Figure 10** presents the BUD geometry on 2D FEM software.

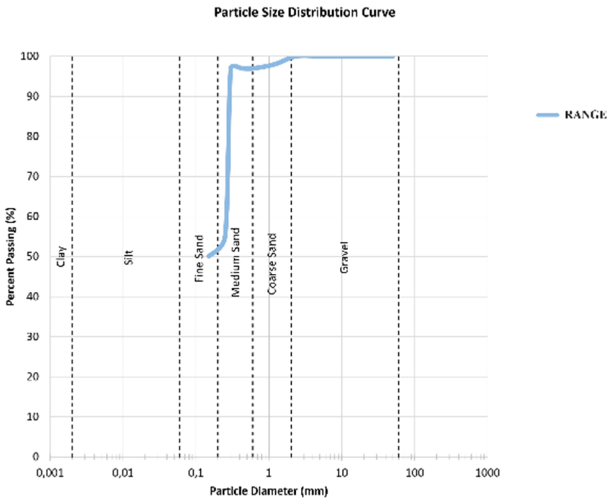

Figure 4 Particle size distribution curve of the tailing dams

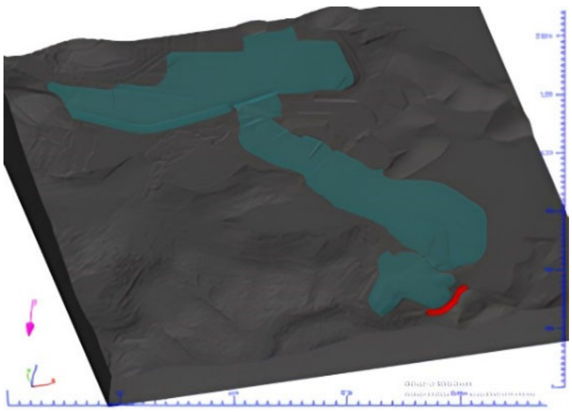

Figure 5 Geometry evaluated by Flow 3D

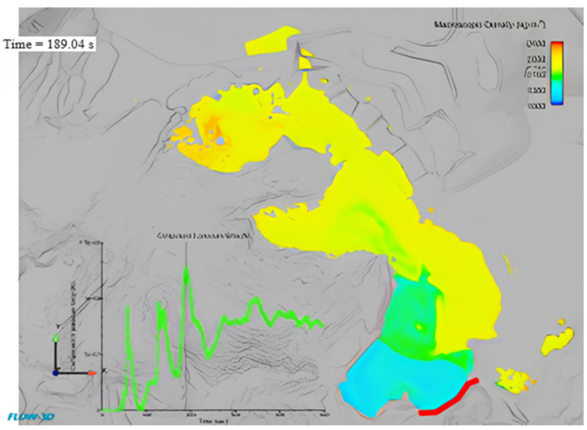

Figure 6 Pressure forces output by Flow3D

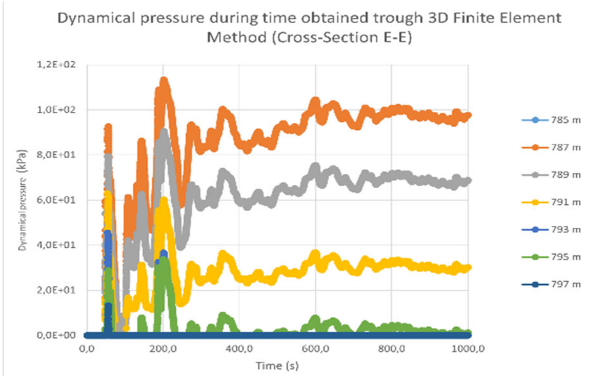

Figure 7 Dynamical pressures over time through 3D FEM in the critical cross-section

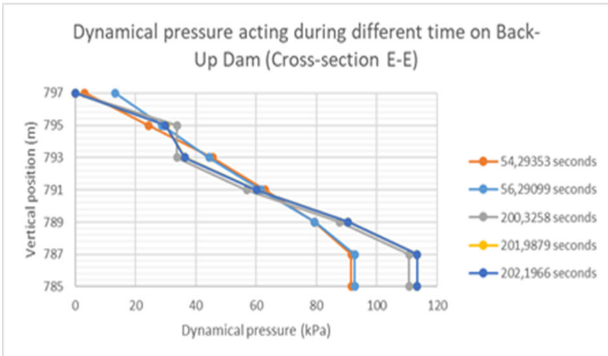

Figure 8 Most significant dynamical loadings acting on the Cross-Section 3D FEM

The concrete between piles has a compressive yielding stress of 15 MPa. Its young modulus is 21 GPa. Two analyses were performed on the BUD taking into consideration the fragile behavior of the concrete: one analysis considering the concrete in an intact state, and one analysis considering the concrete fissured in the region in contact with the pile. The fissured strength parameters were set as 1/3 of the non-fissured strength and the Young modulus was set at 354 MPa.

This Young modulus in an extrapolation of the concrete stress-strain curve in the Brazilian concrete standard NBR6118 (2014), assuming its' strain would be of 3%. **Eq. (3)** is the consideration for the elasticity modulus of the fissured region.

$$E_{cs} = \frac{0{,}85 * f_{ck}}{\gamma_c * \varepsilon} \quad (3)$$

f_{ck}= concrete's compressive yielding stress (MPa); γ_c= resistance reduction coefficient (1,2 to exceptional loading conditions); ε= material's strain (adopted as 3%)

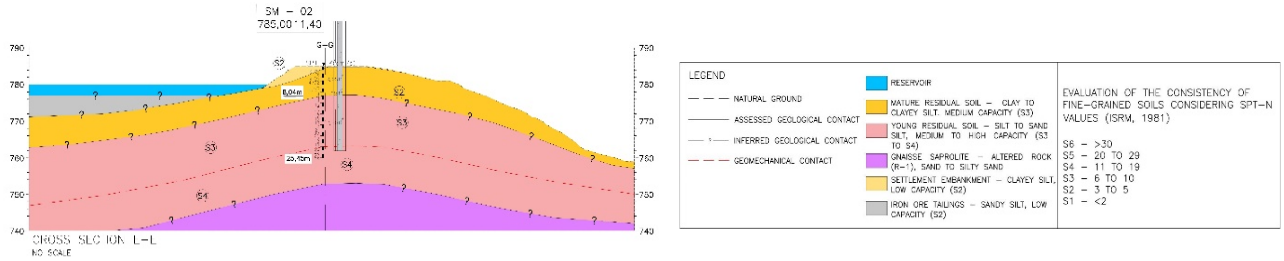

Figure 9 Cross-Section E-E in meters (critical cross-section on the BUD in terms of impact loadings)

3. Results

The analysis of the critical conditions in the model was performed in terms of maximum displacement, angular deflection and bending moment acting on both line 1 (upstream) and line 2 (downstream) during impact loading. The conditions were studied for intact concrete and damaged concrete and are shown in **Figures 11** to **14**.

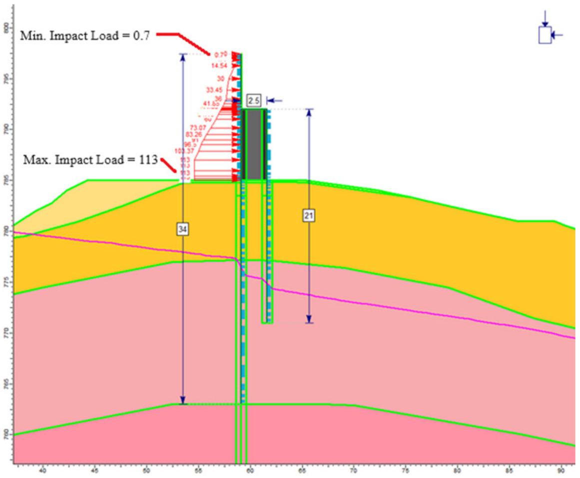

Figure 10 Cross-Section E-E in meters (BUD geometry and impact loadings (kPa) acting on it)

Polynomial equations for the total displacement were set and differentiated to predict angular deflections and bending moments on the piles, following the same method used on Santos and Futai (2022).

The results point out that in terms of structural loadings and deformability limits, the structure is safe. In addition, it shows that the behavior of the BUD with intact concrete and with damaged concrete was very similar. It's understood by these similarities that the stresses are transmitted between piles in a very similar manner, which shows that the concrete is effective in its function.

Figures 15 to **18** show the yielded elements and maximum shear strain on the soil media during impact loading. The maximum shear strain limit was set a 5% considering the research of Matsui and San (1992) that points out that a 5% shear strain acting on a slope could be considered as a shear failure in the region.

The BUD has no probable failing surfaces that should be taken into consideration, since there are no regions near the structure that have shear strains coupled with yielded elements. The region upstream the structure could be failing, but its failure would not be relevant to the general behavior of the BUD.

During the pile driving of the structure, the SILENT PILER equipment generated reports of Rotational Torque, Press-in Force, Extraction Force and Water Jet Volume. These reports underwent statistical analysis of the parameters by layer and depth, in order to establish a data basis for future projects. This statistical analysis was presented in Santos et. al. (2022), with a Kogomorov-Smirnov Test on each variable for curve-fitting to a normal and lognormal distribution. The study showed good results to soil depths of 9m and deeper for the pile line 1 and depths of 7m and deeper for the pile line 2. **Figure 19** presents the Rotational Torque data that fitted to lognormal distribution plotted by depth. **Figure 20** shows the piling operation.

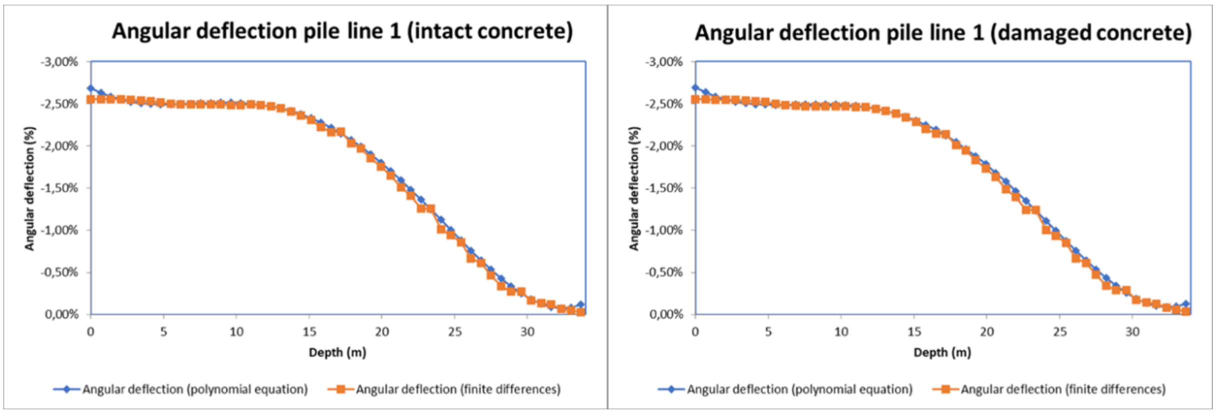

Figure 11 Angular deflection on pile line 1 of BUD Cross-Section E-E during impact loading (intact concrete on the left, damaged concrete on the right)

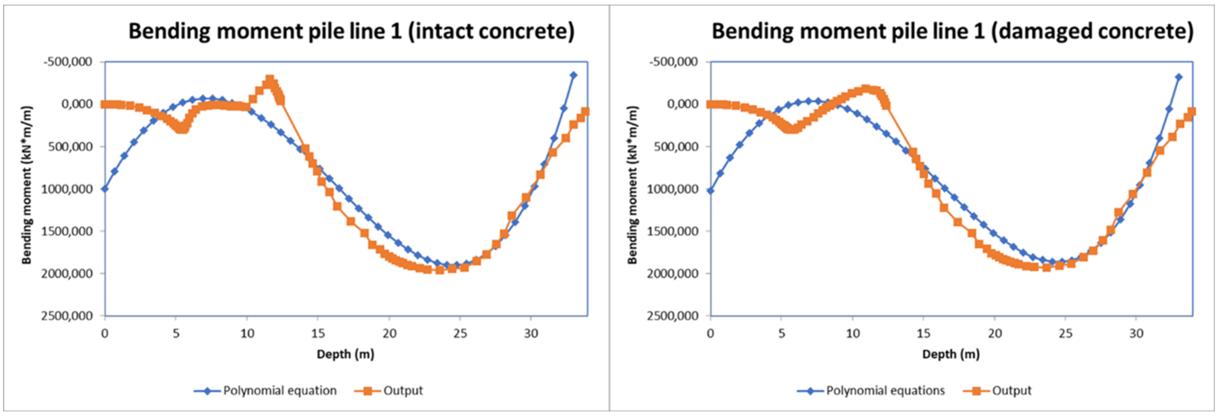

Figure 12 Bending moments on pile line 1 of BUD Cross-Section E-E during impact loading (intact concrete on the left, damaged concrete on the right)

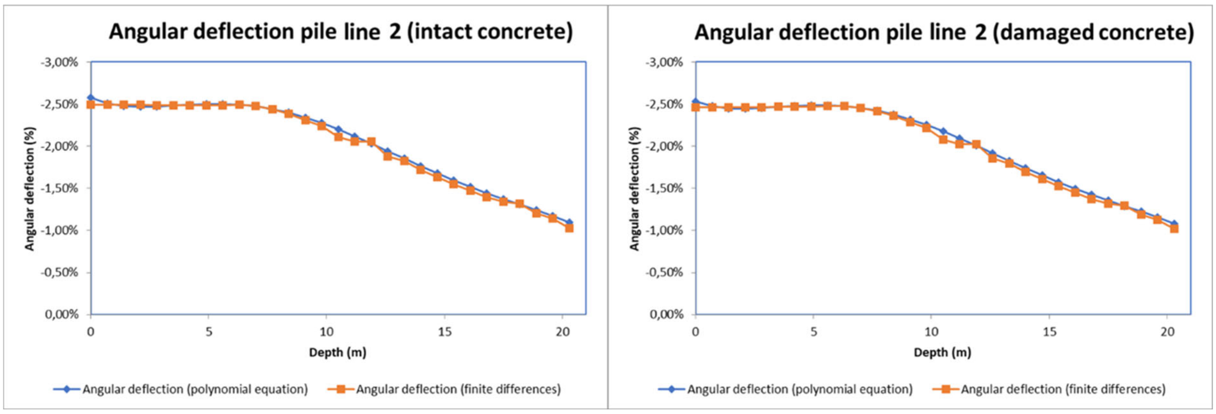

Figure 13 Angular deflection on pile line 2 of BUD Cross-Section E-E during impact loading (intact concrete on the left, damaged concrete on the right)

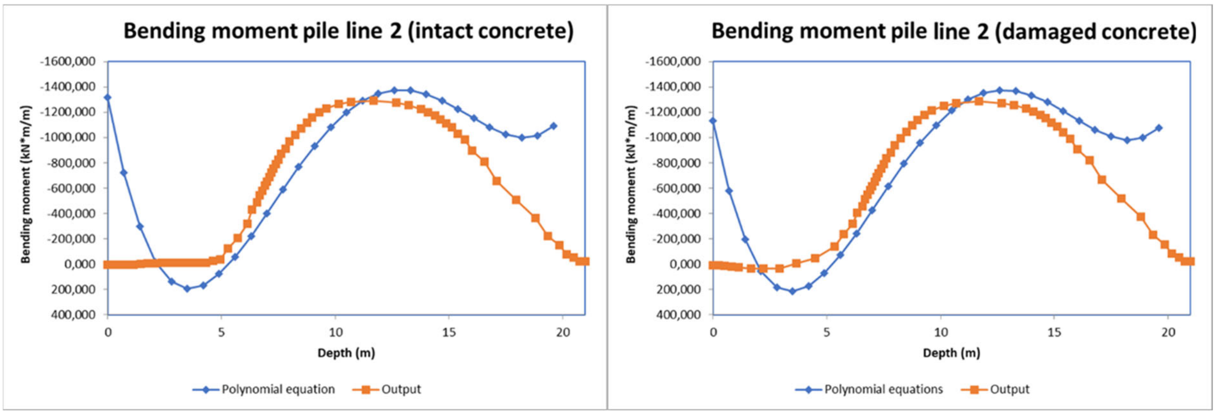

Figure 14 Bending moments on pile line 2 of BUD Cross-Section E-E during impact loading (intact concrete on the left, damaged concrete on the right)

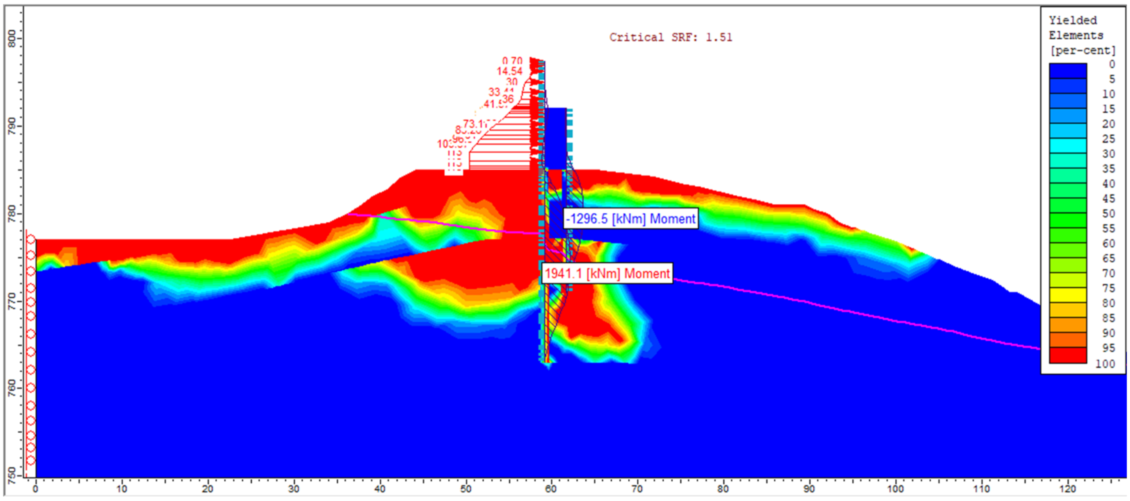

Figure 15 Yielded elements on Cross-Section E-E during impact loading (intact concrete case)

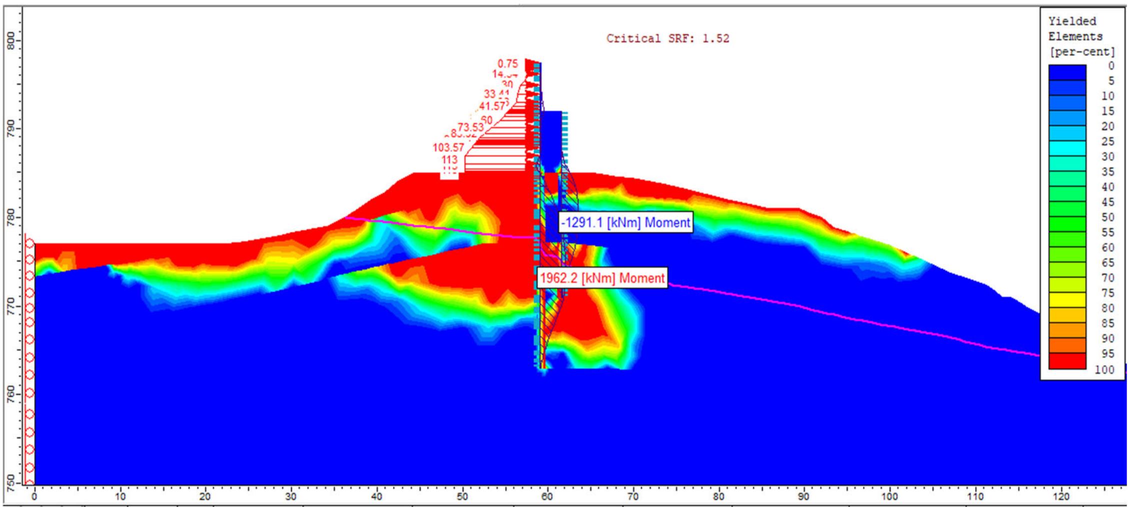

Figure 16 Yielded elements on Cross-Section E-E during impact loading (damaged concrete case)

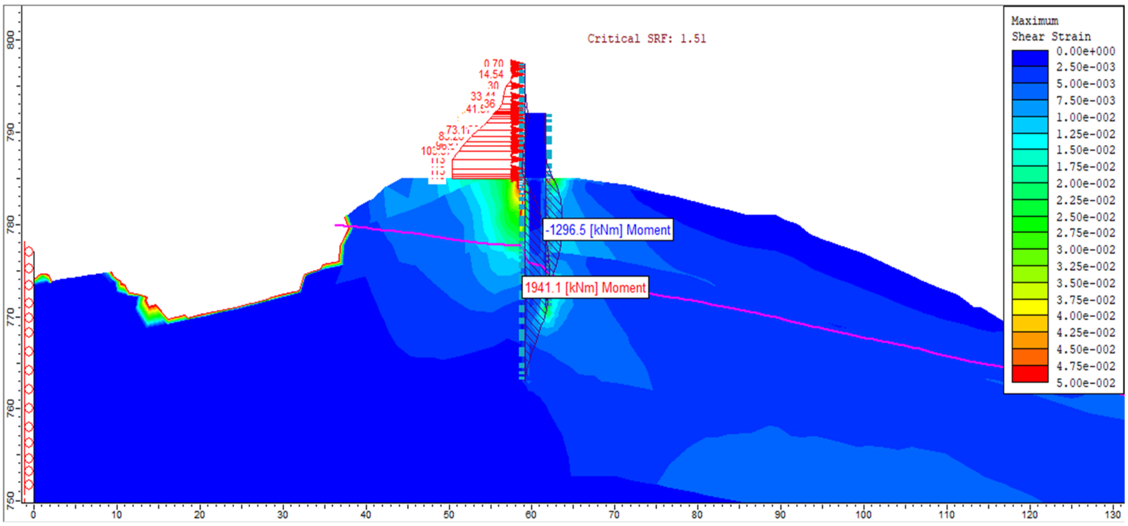

Figure 17 Maximum shear strain on Cross-Section E-E during impact loading (intact concrete case)

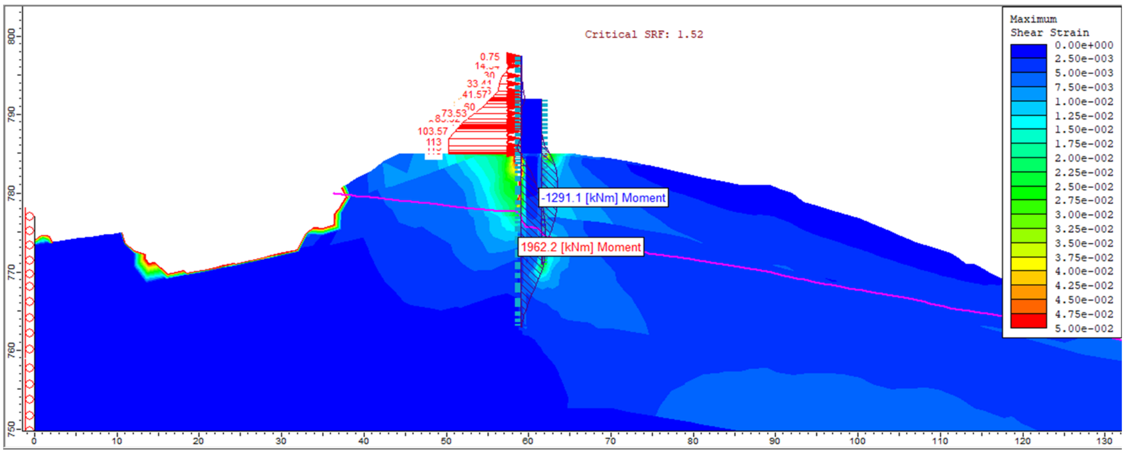

Figure 18 Maximum shear strain on Cross-Section E-E during impact loading (damaged concrete case)

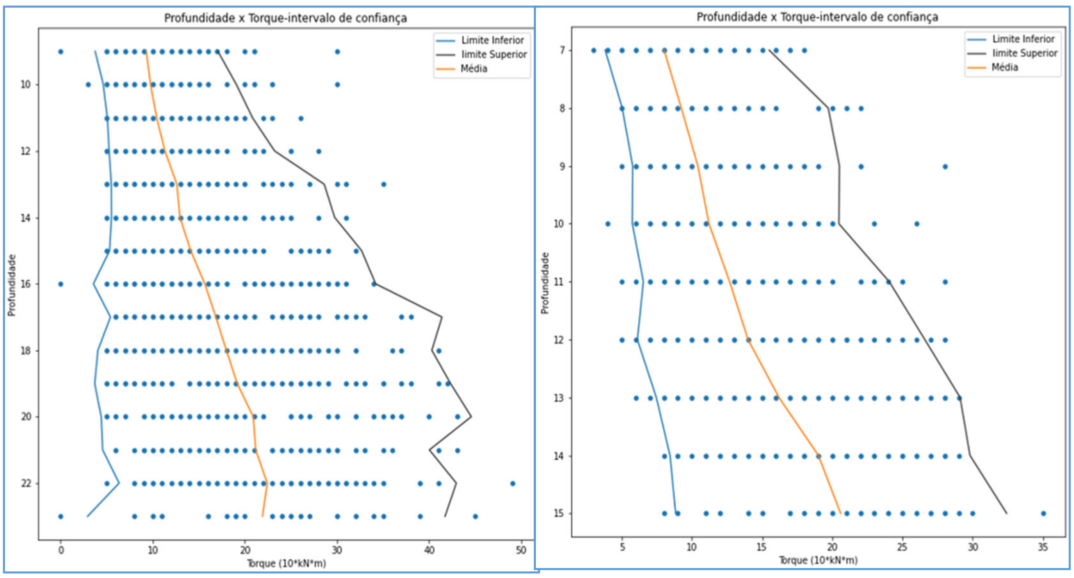

Figure 19 Rotational Torque data that fitted lognormal distribution by depth (on the left, pile line 1; on the right, pile line 2; blue line is the lower limit of the distribution, orange line is the average of the distribution and grey line is the upper limit of the distribution)

Figure. 20 Photograph of the piling operation

4. Conclusions

This paper presents a case study of a structure to withstand the impact loadings of iron ore tailings from a dam that could fail by liquefaction triggering. The study provides structural analysis as well as displacement analysis in order to assess the stability of the structure. Through 3D Finite Element method, it was possible to determine the loadings from the tailings which served as input for the 2D Finite Element method analysis conducted on geotechnical software.

This study also highlights the usage of concrete as a means to transmit stresses between lines of piles on the back up dam and the effects of reducing its resistance and increasing its deformability. Overall, even with a damaged concrete, the transmission of stresses was possible.

This innovative methodology to build a Back Up Dam is an interesting alternative for overcoming the issue of space limits, since this slender structure is able to withstand impact loadings of several 100 kN.

References

Associação Brasileira de Normas Técnicas (2014). ABNT NBR 6118 - 2014. Projeto de estruturas de concreto – Procedimento

Baltazar, O.F.; Baars et. al. (2005) – "Projeto Geologia do Quadrilátero Ferrífero – Integração e Correção Cartográfica em SIG com nota explicativa" CODEMIG. Belo Horizonte

Cheng, X.et al. (1997). Finite element methods for Timoshenko beam, circular arch and Reissner-Mindlin plate problems. Journal of Computational and Applied Mathematics

Ishihara, Yukihiro; Haigh, Stuart. (2018). – "Cambridge Giken Collaborative Working on Pile soil Interaction Mechanisms", Proceedings of the First International Conference on Press-in Engineering, Kochi

Japan Road Association (2009). Standard, ISBN-10: 488950415X 道路土工ー切土工・斜面安定工指針 (Guidelines to roads' earthwork and slope stabilization)

Resolução Conjunta SEMAD/FEAM. Resolução Nº 2.784, de 21 de março de 2019. (2019) – "Determina a descaracterização de todas as barragens de contenção de rejeitos e resíduos, alteadas pelo método a montante, provenientes de atividades minerárias, existentes em Minas Gerais e dá outras providências". Minas Gerais

Santos, G.O.F. et al. (2022). – "Compatibilização de perfil geológico-geotécnico com tratamento de dados de output de estacas cravadas com equipamento Silent Piler em estrutura de contenção a jusante". Revista Brasileira de Engenharia de Barragens, n. 12

Santos, G.O.F.; Futai, M.M. (2022). "Avaliação de critérios de deformabilidade para estruturas de contenção a jusante compostas por estacas tubulares". VIII Conferência brasileira sobre estabilidade de encostas